

## High-Purity Separation of Gold Nanoparticle Dimers and Trimers

Gang Chen,<sup>†</sup> Yong Wang,<sup>†</sup> Li Huey Tan,<sup>†</sup> MiaoXin Yang,<sup>†</sup> Lee Siew Tan,<sup>†</sup> Yuan Chen,<sup>‡</sup> and Hongyu Chen<sup>\*†</sup>

Division of Chemistry and Biological Chemistry and Division of Chemical and Biomolecular Engineering, Nanyang Technological University, Singapore 637371

Received February 2, 2009; E-mail: hongyuchen@ntu.edu.sg

Rational assembly of nanocomponents is the first-step toward scalable fabrication of nanodevices, just as coupling chemistry is to natural product synthesis. Specific clustering of two or three nanoparticles (NPs) by solution methods has been a major challenge, as a nanoassembly must neither dissociate nor aggregate during isolation and application.<sup>1</sup> While our recent work has overcome this difficulty by encapsulating the assembled AuNP clusters (AuNP<sub>n</sub>) with polystyrene-block-poly(acrylic acid) (AuNP<sub>n</sub>@PSPAA),<sup>2</sup> the synthesis of the nanoassemblies is still imperfect without the isolation of high-purity products.

As in organic chemistry, an efficient purification method allows access to selective products from a nonideal synthesis;<sup>3,4</sup> this is particularly important for isolating particle clusters formed by random aggregation.<sup>2,3</sup> The elegant separation of microsphere clusters ( $d \sim 1 \mu\text{m}$ , 2–13 particles) by Pine et al. using density gradient centrifugation demonstrated the precise selectivity of this method comparable to that of chromatography.<sup>3</sup> Very recently, Dai and co-workers reported the use of related methods for separating particles as small as FeCo@C (1–7 nm) and AuNPs (5–20 nm).<sup>5</sup> The clean partition of 5, 10, and 20 nm AuNPs proved the effectiveness of this method for NP purification. In comparison, separating NP clusters such as monomers, dimers, and trimers is conceivably more challenging, considering the small volume (i.e., weight) difference among them (1:2:3 as opposed to 1:8:64 in the above case). Here, we report the isolation of AuNP dimers in high purity (95.1% out of 1435 particles surveyed) by exploiting the high density of CsCl solutions.

Amphiphilic diblock copolymers (e.g., PS<sub>154</sub>PAA<sub>60</sub>) have been shown to self-assemble on AuNPs that were surface-functionalized by hydrophobic ligands.<sup>6,7</sup> The resulting AuNP@PSPAA dispersed well in 100 mM aq. NaCl at neutral pH,<sup>8</sup> considerably more stable than most unprotected NPs. The polymer shell surface is covered with long ionic chains in an extended conformation,<sup>9</sup> which introduce charge and steric repulsion against aggregation. However, these core-shell NPs precipitated at higher salt concentrations, likely owing to the shielding of interparticle charge repulsion at elevated ionic strength. Fortunately at high pH (>10), they were found to tolerate saturated NaCl or CsCl solutions (62% wt, 1.9 g·cm<sup>-3</sup>); even the pelleted NPs after centrifugation readily redispersed. As the PAA only partially deprotonates at neutral pH to minimize charge density in the polymer chain,<sup>10</sup> further deprotonation may have occurred at high pH, providing sufficient surface charge against aggregation. To our knowledge, this is the first report of a colloid stable under such adverse conditions. It allows the use of high-density CsCl solutions for separating heavy nanocrystals like AuNPs.

Another key requirement for isolating high-purity nanoclusters is to prepare NPs of monodispersed size, since a NP 25% larger in diameter is twice in volume. We chose the 15 nm AuNPs (14.6 ± 1.6) prepared by citrate reduction<sup>11</sup> for its narrow size distribution (Figure S6). A random aggregation method was then used to synthesize

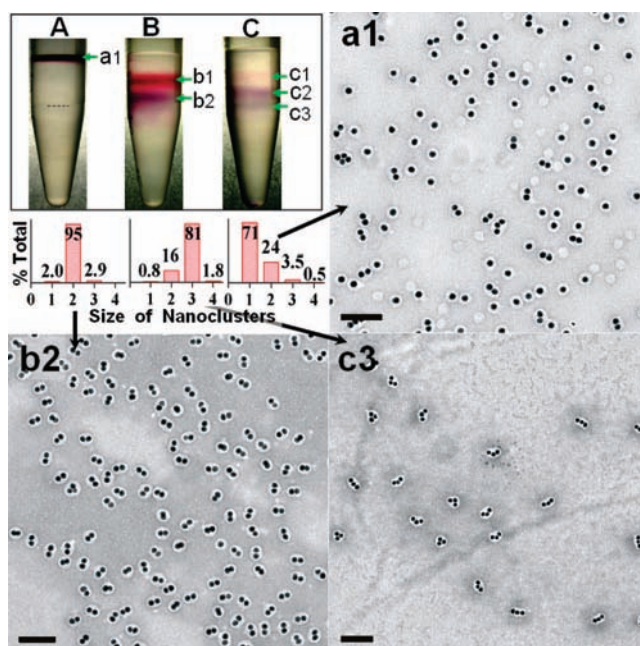


**Figure 1.** (A) A typical setup of differential centrifugation, where 62% and 11% aq. CsCl and then AuNP<sub>n</sub>@PSPAA in water were layered from bottom to top. (B) The result of A after 20 min centrifugation. (C) Separation result of a pre-enriched trimer sample. (a1, b2, and c3) TEM images of the respective fractions indicated in A–C (see large-area views in the Supporting Information); the histograms are shown in the insets. Scale bars: 100 nm.

small clusters: AuNPs surface-functionalized with 2-naphthalenethiol were induced to linearly aggregate by NaCl, and the solution species was preserved by polymer encapsulation and finally isolated by centrifugation (see details in the Supporting Information). To facilitate separation, the aggregation was usually terminated before significant formation of large clusters ( $n \geq 4$ ). The as-synthesized product was typically a mixture consisting of 71% AuNP<sub>1</sub>, 24% AuNP<sub>2</sub>, 3.5% AuNP<sub>3</sub>, and 0.5% AuNP<sub>4</sub> (Figure 1, a1).

To partition the AuNP<sub>n</sub>@PSPAA, a concentrated NP solution was carefully overlaid atop the 11 + 62% CsCl gradient, and the solution was then centrifuged in a desktop microcentrifuge at 8500 rpm (5800 *g*) for 20 min. The resulting solution showed two distinct bands of red and purple color, separated by a gap (Figure 1B). The b2 band was extracted, purified to remove the excess CsCl, and then characterized by TEM. In this sample, dimers amount to 85%. A further purification by the same method enriched the dimers to 95.1% among 1435 particles (monomers and nanoclusters) surveyed (Figure 1, b2). Isolation of trimers is more difficult owing to its low synthetic yield. To enrich trimers, the remaining components after extracting most monomers and dimers were combined and excess CsCl was removed. This sample was then used for a further separation in the 11 + 62% CsCl gradient. The result showed three faint bands of red, purple, and blue color, respectively (Figure 1C). A small aliquot extracted from the c3

<sup>†</sup> Division of Chemistry and Biological Chemistry.

<sup>‡</sup> Division of Chemical and Biomolecular Engineering.

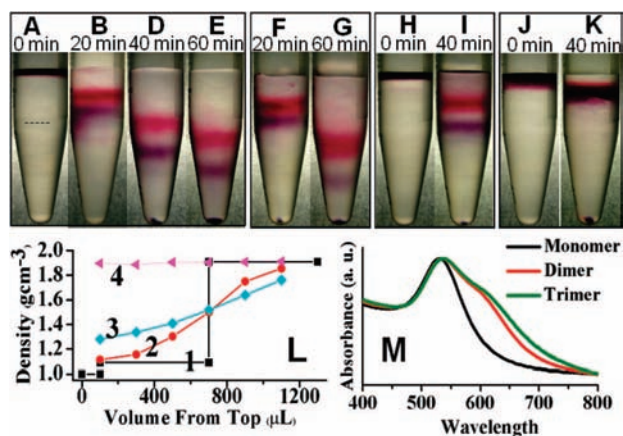


**Figure 2.** (A, B, D, E) Separation of AuNP<sub>n</sub>@PSPAA by differential centrifugation, before (0 min) and after 20, 40, and 60 min. (F, G) All conditions are same as those for B and E, except that the CsCl gradient was precentrifuged for 20 min before loading AuNP<sub>n</sub>@PSPAA. (H, I) AuNP<sub>n</sub>@PSPAA was loaded on top of 62% CsCl solution, before and after 40 min centrifugation. (J, K) AuNP<sub>n</sub>@PSPAA was loaded on top of 50% sucrose solution, before and after 40 min centrifugation. (L) Density trace of the 11 + 62% gradient before (line 1) and after 20 and 120 min (line 2 and 3) centrifugation and density trace of solution I (line 4). (M) UV-vis spectra of monomer, dimer, and trimer samples.

band showed ~81% trimer (out of 1560 particles). Enhancing this purity has been difficult, possibly because the total-AuNP-weight distribution of trimers has significantly overlapped with that of dimers and tetramers (Figure S6). There are ~6.8 dimers per trimer in the as-synthesized sample; if 3% dimers are overweighted ( $m_{\text{AuNP2}} \cong m_{\text{AuNP3}}$ ), ~0.2 dimers (~16.7% of total) will be coseparated with each trimer. In comparison, sample c3 of Figure 1 contained 16% dimers. A narrower size distribution of NPs is, therefore, a prerequisite for further improvements.

The distinct colors of the NP bands are evident from the UV-vis spectra (Figure 2M). In addition to the 530 nm peak that results from transverse plasmon absorption, a dimer sample (85%) showed a clear longitudinal peak at 600 nm, which roughly fit the expected value for gold nanorods of an aspect ratio of 2.<sup>12</sup> In a trimer sample (64%), this peak shifted to 610 nm. Since the trimers often have a bent shape (Figure 1, c3), their spectra are not directly comparable with a gold nanorod of an aspect ratio of 3.

Upon longer centrifugation, both the monomer and dimer bands shifted downward, while the gap between them increased (Figure 2A–E). Clearly, the NPs did not reach equilibrium positions in the density gradient as in the isopycnic centrifugation, and the separation was likely a result of the different sedimentation velocity of various nanoclusters. The sedimentation of monomers even in saturated CsCl solution (Figure 2H–I, vide infra) clearly demonstrated the higher averaged density of AuNP<sub>n</sub>@PSPAA than that of the media ( $\rho_{\text{NP}} > \rho_{\text{solvent}}$ ), further confirming the above conclusion. Density measurement of the solution after centrifugation showed that the original sharp gradient has considerably leveled out even after 20 min and continues to flatten upon longer centrifugation (Figure 2L). The positions of the NP bands are, therefore, largely independent of any sharp density gradient at particular positions. In control experiments where the sharp density gradient was reduced by precentrifuging the 11 + 62% CsCl solution for 20 min, the separation was not substantially affected (Figure 2F–G). It appears that the diffusion of CsCl/H<sub>2</sub>O in a sharp gradient did not contribute significantly to the sedimentation rate difference between monomers and dimers.

Our separation conditions were optimized based on the above understandings: (a) a single density boundary was used to set up the gradient; (b) the top 11% CsCl layer has enough density to reduce

mixing during the addition of aq. AuNP<sub>n</sub>@PSPAA; and (c) the AuNP<sub>n</sub>@PSPAA was loaded in a minimum volume so that the NPs begin sedimentation from the same position.

For a NP under centrifugation,  $f_{\text{friction}}$  should be equal to the difference of  $f_{\text{centrifugal}}$  and  $f_{\text{buoyancy}}$ ; this could be rewritten as

$$fv = m\omega r^2 - m\omega r^2(\rho_{\text{solvent}}/\rho_{\text{NP}})$$

where  $f$  is the frictional coefficient,  $v$  is the steady-state sedimentation velocity,  $m$  is the mass of NP,  $\omega$  is the angular velocity, and  $r$  is the distance from the center of rotation. The  $f_{\text{centrifugal}} - f_{\text{buoyancy}}$  term is understandably larger for a dimer than for a monomer, since a dimer has almost twice the mass of a monomer and a higher density. On the other hand, the frictional coefficient,  $f$ , should be larger for a dimer due to the increased averaged cross section, although it would not be twice as large as that of a monomer considering the equal cross section along the width. This explains why the sedimentation velocity of a dimer is larger than that of a monomer in any solvent, as long as  $\rho_{\text{solvent}} < \rho_{\text{NP}}$ . However, our previous separation in water did not lead to partitions of the nanoclusters.<sup>2</sup>

In contrast to water, both the higher density and viscosity of the CsCl solution could slow down the nanoclusters and, thus, enhance the *relative* difference in the sedimentation velocity. Since  $f_{\text{friction}}$  is proportional to  $v$ , it impedes heavy NPs more than it does light ones. In a 62% CsCl solution of uniform density and viscosity, the sedimentation of AuNP<sub>n</sub>@PSPAA still led to effective separation (Figure 2H–I), indicating that a gradient is not essential in our system. On the other hand, the nanoclusters were only partially separated after 40 min of centrifugation in a 50% sucrose solution (Figure 2J–K), which has a lower density but higher viscosity than the 62% CsCl solution. These results are consistent with the above analysis that  $f_{\text{buoyancy}}$  contributes more to the sedimentation rate difference than  $f_{\text{friction}}$  does.

The encapsulation of various NPs by PSPAA has already been demonstrated;<sup>7,8,13</sup> it is conceivable that our differential centrifugation method could be applied to these NPs. Most importantly, our unique approach has allowed us to separate AuNP dimers and trimers in excellent purity. Since structural intactness is critical for the construction of any nanoassembly, our approach offers a facile separation method without additional inconvenience.

**Acknowledgment.** The authors thank Dr. Haiyan Xu for the simulation in Figure S6 and financial support from MOE (ARC 27/07).

**Supporting Information Available:** Details for synthesis and characterization; large-area views of TEM images. This material is available free of charge via the Internet at <http://pubs.acs.org>.

## References

- (1) (a) Loweth, C. J.; Caldwell, W. B.; Peng, X. G.; Alivisatos, A. P.; Schultz, P. G. *Angew. Chem., Int. Ed.* **1999**, *38*, 1808. (b) Novak, J. P.; Feldheim, D. L. *J. Am. Chem. Soc.* **2000**, *122*, 3979.
- (2) Wang, X. J.; Li, G. P.; Chen, T.; Yang, M. X.; Zhang, Z.; Wu, T.; Chen, H. Y. *Nano Lett.* **2008**, *8*, 2643.
- (3) Manoharan, V. N.; Elsesser, M. T.; Pine, D. J. *Science* **2003**, *301*, 483.
- (4) Khanal, B. P.; Zubarev, E. R. *J. Am. Chem. Soc.* **2008**, *130*, 12634.
- (5) Sun, X. M.; Tabakman, S. M.; Seo, W. S.; Zhang, L.; Zhang, G. Y.; Sherlock, S.; Bai, L.; Dai, H. J. *Angew. Chem., Int. Ed.* **2009**, *48*, 939.
- (6) Kang, Y. J.; Taton, T. A. *Angew. Chem., Int. Ed.* **2005**, *44*, 409.
- (7) Chen, H. Y.; Abraham, S.; Mendenhall, J.; Delamarre, S. C.; Smith, K.; Kim, I.; Batt, C. A. *ChemPhysChem* **2008**, *9*, 388.
- (8) Yang, M. X.; Chen, T.; Lau, W. S.; Wang, Y.; Tang, Q. H.; Yang, Y. H.; Chen, H. Y. *Small* **2009**, *5*, 198.
- (9) Zhang, L. F.; Barlow, R. J.; Eisenberg, A. *Macromolecules* **1995**, *28*, 6055.
- (10) Nagasawa, M.; Murase, T.; Kondo, K. *J. Phys. Chem.* **1965**, *69*, 4005.
- (11) Frens, G. *Nat. Phys. Sci.* **1973**, *241*, 20.
- (12) Link, S.; Mohamed, M. B.; El-Sayed, M. A. *J. Phys. Chem. B* **1999**, *103*, 3073.
- (13) (a) Kang, Y. J.; Taton, T. A. *J. Am. Chem. Soc.* **2003**, *125*, 5650. (b) Kim, B. S.; Qiu, J. M.; Wang, J. P.; Taton, T. A. *Nano Lett.* **2005**, *5*, 1987. (c) Kim, B. S.; Taton, T. A. *Langmuir* **2007**, *23*, 2198.

JA900809Z